This article has been accepted for publication in a future issue of this journal, but has not been fully edited. Content may change prior to final publication. Citation information: DOI 10.1109/TBME.2016.2630009, IEEE Transactions on Biomedical Engineering

EMG-driven optimal estimation of subject-specific Hill model muscle-tendon parameters of the knee joint actuators

A. Falisse, S. Van Rossom, I. Jonkers and F. De Groote

***Abstract— Objective:* The purpose of this paper is to propose an optimal control problem formulation to estimate subject-specific Hill model muscle-tendon (MT-) parameters of the knee joint actuators by optimizing the fit between experimental and model-based knee moments. Additionally, this paper aims at determining which sets of functional motions contain the necessary information to identify the MT-parameters. *Methods:* The optimal control and parameter estimation problem underlying the MT-parameter estimation is solved for subject-specific MT-parameters via direct collocation using an electromyography-driven musculoskeletal model. The sets of motions containing sufficient information to identify the MT-parameters are determined by evaluating knee moments simulated based on subject-specific MT-parameters against experimental moments. *Results:* The MT-parameter estimation problem was solved in about 30 CPU minutes. MT-parameters could be identified from only seven of the 62 investigated sets of motions, underlining the importance of the experimental protocol. Using subject-specific MT-parameters instead of more common linearly scaled MT-parameters improved the fit between inverse dynamics moments and simulated moments by about 30 % in terms of the coefficient of determination (from $\mathbf{0.57 \pm 0.20}$ to $\mathbf{0.74 \pm 0.14}$) and by about 26 % in terms of the root mean square error (from $\mathbf{15.98 \pm 6.85}$ Nm to $\mathbf{11.85 \pm 4.12}$ Nm). In particular, subject-specific MT-parameters of the knee flexors were very different from linearly scaled MT-parameters. *Conclusion:* We introduced a computationally efficient optimal control problem formulation and provided guidelines for designing an experimental protocol to estimate subject-specific MT-parameters improving the accuracy of motion simulations. *Significance:* The proposed formulation opens new perspectives for subject-specific musculoskeletal modeling, which might be beneficial for simulating and understanding pathological motions.**

***Index Terms*—Hill model, Musculoskeletal modeling, Optimal control, Parameter estimation, Parameter identification**

I. Introduction

Human motions can be simulated using musculoskeletal models that reproduce the muscle-tendon (MT-) force distribution and translate it into skeletal motions. The MT-force distribution is calculated from the MT-dynamics that comprise activation and contraction dynamics describing the nonlinear relations between muscle excitation and muscle activation and between muscle activation and MT-force respectively. The contraction dynamics can be represented by the Hill model [1] that defines the force generating capacity of a MT-actuator based on five MT-parameters: the maximal isometric muscle force $F_m^{\max}$, the optimal muscle fiber length l_m^{opt}, the tendon slack length l_t^s, the maximal muscle fiber velocity $v_m^{\max}$, and the optimal pennation angle α^{opt}. The MT-parameters are difficult to estimate from *in vivo* measurements and are mostly compiled from cadaver studies [2]–[4]. Different methods then exist to scale these generic parameters based on the subject's anthropometry. Although linear scaling is common, scaling methods that preserve the muscle operating range, such as proposed by Winby *et al.* [5] and recently generalized by Modenese *et al.* [6], have been shown to be more accurate. Yet the MT-properties are known to vary with age, gender, and activity level [7], [8]. They are hence subject-specific and cannot be truly estimated based on anthropometrical dimensions only. In this study, we therefore rely on a functional approach (i.e. based on experimental angle-moment relationships) to estimate subject-specific MT-parameters. In particular, we focus on the estimation of l_t^s and l_m^{opt} as joint moment simulations are most sensitive to those two MT-parameters [9]–[12].

The overall approach to estimate subject-specific parameters based on a functional approach is to minimize the difference between experimental and model-based joint moments by optimizing the parameters. Such an approach was used to determine subject-specific torque-angle-angular velocity relationships [13] and subject-specific MT-parameters. In the second case, we can distinguish approaches based on maximal and sub-maximal muscle contraction that rely on angle-moment relationships measured during isometric dynamometry [14]–[16] and functional motions [17], [18] respectively. Isometric dynamometry, however, has several limitations, restricting its use for estimating MT-parameters. First, a complete and large set of measurements is difficult to obtain, since it requires many maximal voluntary contractions leading to a lengthy protocol and requiring substantial effort from the test subject which may cause fatigue [15], [16]. Second, maximal muscle contraction is practically never reached [19], limiting the applicability of such approaches as illustrated by Wesseling *et al.* [20]. For these reasons, we selected a sub-maximal contraction-based approach to estimate subject-specific MT-parameters. Such an approach

This work was supported by an IWT-TBM grant (140184) and a PhD grant of the Research Foundation Flanders (FWO).

All authors are with the Department of Kinesiology, KU Leuven, Tervuursevest 101 bus 1501, 3001 Leuven, Belgium (correspondence e-mail: antoine.falisse@kuleuven.be).

This article has been accepted for publication in a future issue of this journal, but has not been fully edited. Content may change prior to final publication. Citation information: DOI 10.1109/TBME.2016.2630009, IEEE Transactions on Biomedical Engineering

allows the collection of a rich experimental dataset with standard motion capture equipment. Although muscle excitation is *a priori* unknown in sub-maximal contraction-based approaches, electromyography (EMG) provides a muscle excitation estimate that can drive musculoskeletal models to simulate joint moments during functional motions (e.g. EMG-driven models of the knee [17], [21]). In this study, we use an EMG-driven model to estimate MT-parameters by optimizing the fit between experimental and model-based joint moments. Since the MT-parameter dependent relationship between EMG and joint moments is dynamic, solving the corresponding optimization problem requires the transcription of an infinite-dimensional problem into a finite-dimensional approximation. Estimating the MT-parameters using this approach therefore corresponds to solving an optimal control and parameter estimation problem, also referred to as an optimal estimation problem [22].

The formulation of the MT-parameter estimation problem influences the convergence and efficiency of the numerical optimization. Numerically efficient formulations of the MT-parameter estimation problem were introduced [15], [16], but only for methods based on maximal contraction-based approaches that do not include the MT-dynamics. When considering the MT-dynamics for consistency with muscle physiology, the problem becomes challenging to solve due to the nonlinearity and stiffness of the dynamic equations. A suitable numerical method is therefore required to solve the underlying complex system of differential equations. Direct collocation methods have recently become increasingly popular for the numerical solution of optimal control problems and were used in several human motion simulation studies [23]–[25]. A direct collocation method implicitly takes the system dynamics into account by parametrizing both controls and states, defining a sparse and thus tractable nonlinear programming problem (NLP). Collocation methods are often more computationally efficient than, for example, shooting methods that rely on explicit integration of the dynamic equations [17], [18], [26]. The first aim of this study is to use, for the first time, a direct collocation method to estimate subject-specific MT-parameters, relying on a robust and computationally efficient formulation of the optimal estimation problem [25].

In particular, this study seeks to estimate subject-specific MT-parameters that represent the subject's MT-properties rather than optimize the fit with the experimental data for a set of motions. This is an important requirement when using the subject-specific models in predictive "what if" scenarios that differ from the experimental conditions. Since the information in the experimental dataset determines whether the MT-parameters can be accurately estimated, a careful selection of the experimental dataset is required. When the dataset contains insufficient information, the experimental data can be fitted with high precision while the estimated parameters are inaccurate and hence result in unreliable predictions for motions that were not included in the dataset. This phenomenon is known as overfitting [27]. We thus want to select experimental datasets that can identify the MT-parameters and hence provide valid MT-parameter estimates. The second aim of this study is therefore to investigate the identifiability of the MT-parameters based on different sets of motions. To this end, the accuracy of knee moment simulations based on subject-specific MT-parameters estimated from various sets of motions was evaluated.

In this study, novelty is twofold. First, an optimal estimation problem is formulated to efficiently estimate subject-specific MT-parameters of the knee actuators based on an EMG-driven model. Second, the identifiability of the MT-parameters based on different sets of motions is studied to provide valuable information regarding the experimental datasets needed for their estimation.

II. METHODS

A. Experimental data

Eight healthy volunteers (four males and four females, age 29.8 $\pm$ 3.9 years, height 176 $\pm$ 6.6 cm, and weight 69.6 $\pm$ 6.0 kg) gave informed consent to participate in the study approved by the Ethics Committee at UZ Leuven (Belgium). Each subject was instrumented with 65 retro-reflective skin-mounted markers, corresponding to an extended plug-in-gait marker set, whose three-dimensional locations were recorded (100 Hz) using a ten-camera motion capture system (Vicon, Oxford, UK) during six functional motions: gait, squat, stair descent, stair ascent, sit-to-stand-to-sit, and squat jump. The motions were chosen as they (i) encompass a wide range of contractile conditions, (ii) require large knee moments (up to ∼100 Nm), (iii) require a large range of knee angles (∼-2° to 100° knee flexion), (iv) reflect various MT-force distributions and (v) are easily achievable in practice. In particular, the squat jump motion was included as it requires higher muscle activation. The wide variety of motions was intended to provide a dataset with sufficient information to estimate MT-parameters that truly represent the subject's MT-properties rather than only reproduce the experimental data. Ground reaction forces (GRF) and EMG data were recorded (1000 Hz) using force plates (AMTI, Watertown, USA) and wireless EMG acquisition systems (ZeroWire EMG Aurion, Milano, Italy) respectively. GRF were low-pass filtered (10 Hz) using a fourth-order Butterworth filter. EMG data were collected from six muscle groups of each leg (Table 1) and were processed by band-bass filtering (20-400 Hz), full-wave rectification, and low-pass filtering (10 Hz) using a fourth-order Butterworth filter. EMG data were also collected during maximum voluntary contraction (MVC) trials and processed using the same protocol. To robustly determine the maximal EMG values, a centered moving average with a 50 ms time window was applied to the processed EMG data of both functional motions and MVC trials. The resulting peak values were then used to normalize the EMG envelopes [28]. Based on the quality of the normalized EMG envelopes, 11 experimental datasets (seven left and four right legs) were selected.

B. Musculoskeletal model and data processing

The experimental data were processed in OpenSim 3.2 [29] based on the gait2392 musculoskeletal model containing 20

TABLE I
ASSIGNMENT OF EMG ENVELOPES TO THE MODEL'S KNEE ACTUATORS

Experimental EMG envelopes	Model's knee actuators
Hamstring lateralis	Biceps femoris long head (BFLH) Biceps femoris short head (BFSH)
Gastrocnemius lateralis	Gastrocnemius lateralis (GL) Gastrocnemius medialis (GM)
Hamstring medialis	Semimembranosus (SM) Semitendinosus (ST) Sartorius (SA) Gracilis (GR)
Rectus femoris	Rectus femoris (RF)
Average(vastus lateralis, vastus medialis)	Vastus intermedius (VI)
Vastus lateralis	Vastus lateralis (VL)
Vastus medialis	Vastus medialis (VM)

segments and 23 degrees of freedom (DOFs) [2]. The marker-based knee axis of this model was replaced by a functional axis, estimated based on knee flexion-extension measurements [30]. Each knee joint was actuated by 12 MT-actuators ($N = 12$): eight flexors (biceps femoris long head (BFLH), biceps femoris short head (BFSH), sartorius (SA), gastrocnemius lateralis (GL), gastrocnemius medialis (GM), semimembranosus (SM), semitendinosus (ST), and gracilis (GR)) and four extensors (rectus femoris (RF), vastus intermedius (VI), vastus lateralis (VL), and vastus medialis (VM)).

The musculoskeletal model was scaled to the subject's anthropometry using OpenSim's scale tool based on marker information collected during a static trial. This process included linear scaling of l_t^s and l_m^{opt} using a scale factor computed as the ratio of the corresponding MT-actuator's length before and after scaling. This approach therefore preserves the ratio l_m^{opt} to l_t^s. For each functional motion, joint kinematics and moments were calculated based on marker trajectories and GRF by successively applying a Kalman smoothing algorithm for inverse kinematics [31] and an inverse dynamics (ID) analysis via OpenSim. Only knee flexion-extension moments were further considered. MT-lengths and moment arms were computed as a function of the joint kinematics using OpenSim's muscle analysis tool. The EMG envelopes were assigned to the model's knee actuators as described in Table 1. Hamstring lateralis EMG drove both BFLH and BFSH. Hamstring medialis EMG drove SM and ST [18] as well as SA and GR. GM EMG drove both GM and GL, whilst the input of VI was estimated as the average of VL and VM EMG [17], [18]. An electromechanical delay of 40 ms was introduced by time-shifting the EMG envelopes [27].

The MT-dynamics, comprising activation and contraction dynamics, were described by two nonlinear first-order differential equations relating the control, muscle excitation, to the states, neural excitation and normalized muscle fiber length. Activation dynamics were defined based on Thelen [32], [33]:

$$r = f_a(e) \tag{1}$$

where f_a describes the transformation from muscle excitation e to neural excitation r. This equation was augmented with the EMG-to-activation relationship [17], [27] relating neural

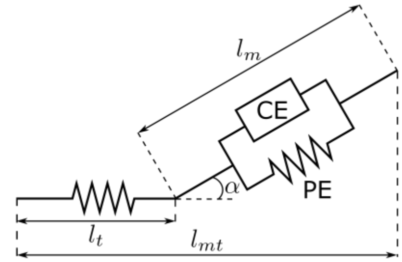

Fig. 1. Schematic representation of the Hill model [1]. The MT-actuator, of length l_{mt}, comprises a tendon in series with a pennate muscle. The tendon is modeled as a nonlinear spring of length l_t. The muscle, of length l_m, consists of a contractile element (CE) parallel to a passive element (PE). The pennation angle α is the angle between the orientation of the muscle fibers and the tendon.

excitation r to muscle activation a:

$$a = \frac{e^{Ar} - 1}{e^{A} - 1}, \tag{2}$$

where A is a nonlinear shape factor. Contraction dynamics were described by the Hill model [1] that defines the MT-actuator as a tendon in series with a pennate muscle. The tendon is modeled as a nonlinear spring of length l_t and the muscle, of length l_m with pennation angle α, consists of a contractile element (CE) in parallel with a passive element (PE) (Fig. 1). The MT-force F_{mt} was given by:

$$F_{\text{mt}} = F_t(\tilde{l}_t) = F_m(a, \tilde{l}_m, \tilde{v}_m) \cos\alpha \tag{3}$$

where F_t is tendon force, which is a function of the normalized tendon length $\tilde{l}_t = l_t/l_t^s$, and F_m is muscle force, which is a function of muscle activation a, normalized muscle fiber length $\tilde{l}_m = l_m/l_m^{\text{opt}}$ and normalized muscle fiber velocity $\tilde{v}_m = v_m/v_m^{\text{max}}$ (see supplementary materials for more details).

C. *Optimal estimation of subject-specific MT-parameters*

The overall process to solve the optimal estimation problem for subject-specific MT-parameters is outlined in Fig. 2a.

1) *Multiple-phase optimal estimation problem*

The subject-specific MT-parameters were estimated based on different sets of motions, later referred to as calibration sets. Each calibration set represents a possible combination amongst the six motions. There exist thus 63 $\left(\sum_{i=1}^{6} 6!/i!\,(6-i)!\right)$ possible calibration sets. For each of these sets, a multiple-phase optimal estimation problem with each phase corresponding to a motion was solved for subject-specific MT-parameters. For example, the calibration set consisting of gait and squat results in a 2-phase optimal estimation problem (phase 1: gait and phase 2: squat) which is solved for the corresponding subject-specific MT-parameters. Solving the optimal estimation problem consisted in determining the controls, states and static parameters (defined in subsection 2) satisfying the constraints imposing the MT-dynamics (subsection 3), the boundary conditions (subsection 4), and the path constraints (subsection 5), while optimizing a cost functional (subsection 6).

2) *Static parameters*

l_t^s and l_m^{opt} of eight ($J = 8$) knee actuators (four flexors: BFLH, GL, GM, SM and four extensors: RF, VI, VL, VM) were

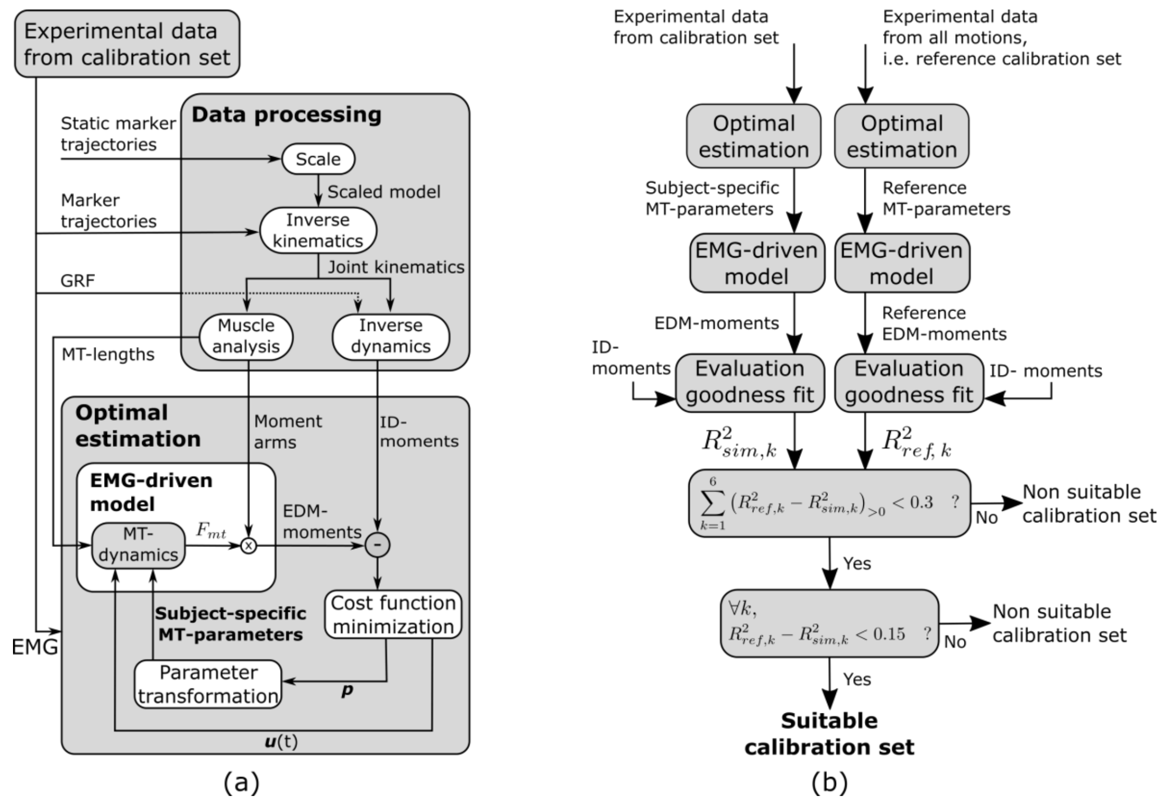

Fig. 2. (a) Flow chart illustrating the process used to estimate the subject-specific MT-parameters. The optimal estimation problem underlying the MT-parameter estimation is solved for the states $\boldsymbol{x}$(t) (defining the MT-force F_{mt}) , controls $\boldsymbol{u}$(t), and static parameters $\boldsymbol{p}$ that minimize the difference between ID- and EMG-driven model-based (EDM-) moments. A parameter transformation is applied to extract the subject-specific MT-parameters from the static parameters. (b) Flow chart illustrating the process used to select the calibration sets that are suitable (i.e. contain sufficient information) to identify the MT-parameters. $k = 1, \ldots, 6$ represents the functional motions.

estimated based on a sensitivity analysis [11]. Values from the linearly scaled models were assigned to the other MT-parameters.

For each knee actuator j $(j = 1, \ldots, J)$, physiologically feasible combinations $[l_{m,j}^{\mathrm{opt}}, l_{t,j}^{s}]$ were defined to constrain the search space of the optimal estimation problem as described by Van Campen *et al.* [16]. Furthermore, to improve the numerical condition of the problem, the ratio $l_{t,j}^{s}/l_{m,j}^{\mathrm{opt}}$ and a parameter δ_j were used as static parameters instead of $l_{t,j}^{s}$ and $l_{m,j}^{\mathrm{opt}}$. The parameter δ_j determines the deviation from the first-order regression of the physiologically feasible combinations $[1/l_{m,j}^{\mathrm{opt}}$, $l_{t,j}^{s}/l_{m,j}^{\mathrm{opt}}$] defined by:

$$\frac{1}{l_{m,j}^{\mathrm{opt}}} - C_{1,j}\frac{l_{t,j}^{s}}{l_{m,j}^{\mathrm{opt}}} - C_{2,j} = \delta_j, \tag{4}$$

where $C_{1,j}$ and $C_{2,j}$ are the regression coefficients [16] (see supplementary materials for more details).

A single nonlinear shape factor A (2) for all muscles was added to the set of static parameters.

3) Constraints imposing the MT-dynamics

The MT-dynamics were formulated as described by De Groote *et al.* [25]. Activation dynamics were imposed using muscle excitation e and neural excitation r as respectively control and state. Contraction dynamics were imposed using normalized muscle fiber length $\tilde{l}_m$ as state and introducing u_v, the scaled time derivative of $\tilde{l}_m$, as a new control simplifying the dynamic equations:

$$\frac{d\tilde{l}_m}{dt} = \frac{v_m^{\max}}{l_m^{\mathrm{opt}}} u_v, \tag{5}$$

where $v_m^{\max}/l_m^{\mathrm{opt}}$ is a scaling factor that converts u_v into $\tilde{v}_m$. The nonlinear equations describing the contraction dynamics were then imposed as algebraic constraints in their implicit form, simplifying their evaluation. Efficiency and robustness of this implicit formulation of the contraction dynamics was previously demonstrated [25].

4) Boundary conditions

States $\boldsymbol{x}(t) = [r_j, \tilde{l}_{m,j}]$, controls $\boldsymbol{u}(t) = [e_j, u_{v,j}]$ and static parameters $\boldsymbol{p} = [l_{t,j}^{s}/l_{m,j}^{\mathrm{opt}}, \delta_j, A]$ were bounded by:

$$0 \leq r_j, e_j \leq 1, \tag{6}$$

$$0.4 \leq \tilde{l}_{m,j} \leq 1.6, \tag{7}$$

$$-1 \leq u_{v,j} \leq 1, \tag{8}$$

$$\left(\frac{l_{t,j}^{s}}{l_{m,j}^{\mathrm{opt}}}\right)^{\min} \leq \frac{l_{t,j}^{s}}{l_{m,j}^{\mathrm{opt}}} \leq \left(\frac{l_{t,j}^{s}}{l_{m,j}^{\mathrm{opt}}}\right)^{\max}, \tag{9}$$

$$\delta_j^{\min} \leq \delta_j \leq \delta_j^{\max}, \tag{10}$$

$$-3 < A < 0. \tag{11}$$

Constraints (6-8) were based on the definition of the Hill model [1], (9-10) followed from the definition of the physiologically feasible combinations and (11) was imposed to limit the variation of the nonlinear shape factor A in the EMG-to-activation relationship [17], [27].

5) Path constraints

Additional path constraints were introduced:

$$-0.01 \leq e_j - EMG_j \leq 0.01, \tag{12}$$

$$0.9 \leq \frac{l_{m,\mathrm{VI}}^{\mathrm{opt}}}{l_{m,\mathrm{VL}}^{\mathrm{opt}}}, \frac{l_{m,\mathrm{VI}}^{\mathrm{opt}}}{l_{m,\mathrm{VM}}^{\mathrm{opt}}}, \frac{l_{m,\mathrm{VL}}^{\mathrm{opt}}}{l_{m,\mathrm{VM}}^{\mathrm{opt}}} \leq 1.1\,, \tag{13}$$

$$0.9 \leq \frac{l_{m,\mathrm{GM}}^{\mathrm{opt}}}{l_{m,\mathrm{GL}}^{\mathrm{opt}}} \leq 1.1. \tag{14}$$

Non-zero bounds were chosen in (12) to allow for small deviations from the measured EMG signals in order to compensate for measurement errors. Only small deviations were permitted to limit the redundancy (a better fit between simulated and ID-moments can be obtained by optimizing either muscle excitation or MT-parameters). Constraints (13-14) were anatomically-informed and respectively enforced that optimal muscle fiber lengths of the three vasti and both gastrocnemii were in the same range [16].

6) Cost functional

The multiple-phase optimal estimation problem was solved by determining, in each phase, the controls $\boldsymbol{u}(t)$, states $\boldsymbol{x}(t)$ and phase-independent static parameters $\boldsymbol{p}$ that minimize the cost functional:

$$L = \int_{t_i}^{t_f} \left(M_{ID}(t) - M_{EDM}(\boldsymbol{u}(t), \boldsymbol{x}(t), \boldsymbol{p})\right)^2 dt, \tag{15}$$

where t is the time, t_i and t_f are the initial and final time, M_{ID} represents the ID-moments, and M_{EDM} represents the EMG-driven model-based (EDM-) moments given by:

$$M_{EDM} = \sum_{j=1}^{J} d_j(t) F_{t,j}\,(\boldsymbol{u}(t), \boldsymbol{x}(t), \boldsymbol{p}) + f, \tag{16}$$

where d_j is the moment arm of knee actuator j. The contribution to the knee moments of the four ($B = 4$) knee actuators whose MT-parameters were not estimated was pre-computed:

$$f = \sum_{\mathrm{b}=1}^{B} d_b(t) F_{t,\mathrm{b}}(EMG(t)), \tag{17}$$

where $F_{t,b}$ was obtained by forward integration of the MT-dynamic equations using the EMG envelope as control.

Finally, to penalize deviation of muscle excitation from the EMG envelope, a penalty function φ was appended to the cost functional:

$$\varphi = w \int_{t_i}^{t_f} \sum_{j=1}^{J} \left(e_j - EMG_j\right)^2 dt, \tag{18}$$

where $w = 1000$ is a parameter that weights the penalty function against the other term in the cost functional.

7) Computational solution

The optimal estimation problem was solved numerically via direct collocation using GPOPS-II optimal control software [34]. The problem was solved on a mesh of 100 intervals per motion using third-order Legendre-Gauss-Radau collocation. The interior point solver IPOPT [35] was used to solve the resulting NLP using second-order derivative information. The derivatives required by the NLP solver were provided by the open-source automatic differentiation software ADiGator [36].

8) Initial guess

To decrease the probability of finding local optima as a consequence of using a gradient-based method, the optimal estimation problem was solved using two initial guesses of static parameters. The first initial guess was based on a pre-computed hot start whereas the second initial guess was arbitrary (see supplementary materials for more details). The solution resulting in the smallest value of the cost functional was then selected.

D. MT-parameter identification

MT-parameters were estimated from each calibration set resulting in 63 estimates of subject-specific MT-parameters per dataset. The motions belonging to the calibration sets will be referred to as calibration motions and the remaining motions as validation motions. For example, when MT-parameters are estimated based on experimental data from gait and squat, the calibration motions are gait and squat and the validation motions are stair ascent, stair descent, sit-to-stand-to-sit and squat jump.

Knee moments (EDM-moments) were computed via forward integration of the MT-dynamic equations using the EMG envelopes as controls for all motions and for the 63 MT-parameter estimates. Two metrics were used to evaluate the goodness of fit between ID- and EDM-moments: the coefficient of determination (R^2) and the root mean square error (RMSE).

The calibration set containing all six motions was chosen as reference calibration set and we refer to the corresponding MT-parameter estimate and EDM-moments as respectively reference MT-parameters and reference EDM-moments. The reference MT-parameters minimize the difference between ID- and EDM-moments over all motions, resulting in the best overall fit but not in the best fit for each individual motion.

The identifiability of the MT-parameters from different calibration sets was assessed by comparing the coefficients of determination calculated between ID- and EDM-moments (R_{sim}^2) to the ones calculated between ID- and reference EDM-moments (R_{ref}^2). Calibration sets for which R_{sim}^2 were similar to R_{ref}^2 for all motions were considered suitable to identify the MT-parameters. The process for selecting the calibration sets that were suitable to identify the MT-parameters is outlined in Fig. 2b. The similarity between R_{sim}^2 and R_{ref}^2 was evaluated based on two criteria: 1) the sum of the positive deviations (i.e. if $R_{\mathrm{ref}}^2 - R_{\mathrm{sim}}^2 > 0$) over all motions was limited to 0.3 and 2) a deviation ($R_{\mathrm{ref}}^2 - R_{\mathrm{sim}}^2$) larger than 0.15 was not allowed for any individual motion. These criteria were chosen to limit the overall deviation from reference EDM-moments as well as the deviation for each individual motion. This second criterion was especially important to prevent overfitting characterized by a good fit for the calibration motions but large deviations for validation motions. In total, subject-specific MT-parameters estimated from 62 calibration sets were investigated and compared to the reference MT-parameters. Calibration sets that were suitable across all 11 datasets were selected. The other calibration sets did not result in valid MT-parameter estimates as they failed to reproduce the joint moments for the validation motions.

The subject-specific MT-parameters were then compared to (i) the reference MT-parameters, (ii) the linearly scaled MT-parameters obtained from OpenSim's scale tool, and (iii) the nonlinearly scaled MT-parameters computed using an anthropometric algorithm recently proposed by Modenese *et al.* [6] (see supplementary materials for more details regarding the implementation of the algorithm).

III. Results

Seven of the 62 investigated calibration sets satisfied both criteria across all 11 datasets and were thus suitable to identify the MT-parameters (calibration sets A-G in Table 2). Gait and sit-to-stand-to-sit were part of all (7/7) suitable calibration sets followed by squat jump (6/7), squat and stair ascent (4/7), and stair descent (3/7).

EMG-driven simulations based on subject-specific MT-parameters yielded more accurate knee moment predictions than simulations based on anthropometry-based scaled MT-parameters (Table 3). The fits between ID- and EDM-moments improved from 0.57 ± 0.20 to 0.74 ± 0.14 in terms of R^2 and 15.98 ± 6.85 Nm to 11.85 ± 4.12 Nm in terms of RMSE using subject-specific MT-parameters rather than linearly scaled MT-parameters. These results are averaged over all six motions, 11 datasets and, for subject-specific MT-parameters, seven suitable calibration sets. Similar observations hold when comparing to the nonlinearly scaled MT-parameters for which the fits were 0.57 ± 0.21 in terms of R^2 and 15.99 ± 6.94 Nm in terms of RMSE when averaged over all six motions and 11 datasets.

Although the subject-specific MT-parameters estimated from the seven suitable calibration sets were not identical, they closely resembled the reference MT-parameters estimated from all motions. For l_t^s and l_m^{opt}, the largest averaged deviations were observed for BFLH (4.5 %) and RF (6.3 %) respectively. Compared to linearly scaled MT-parameters, subject-specific l_t^s of the flexors were smaller (averaged ratio 82.1 ± 10.2 %), subject-specific l_m^{opt} of the flexors were larger (averaged ratio 143.0 ± 25.8 %) and subject-specific l_t^s and l_m^{opt} of the extensors were relatively comparable. Linearly scaled MT-parameters were thus comparable to subject-specific MT-parameters for the extensors, in particular the vasti, but not for the flexors. Similar observations hold when comparing subject-specific MT-parameters to nonlinearly scaled MT-parameters. All ratios are averaged over all seven suitable calibration sets and 11 datasets. Detailed numbers of those analyses are presented in the supplementary materials (Tables S4-S5).

Between 17 and 41 computation (CPU) minutes were required to solve the optimal estimation problem from both initial guesses for the suitable calibration sets (Table 2).

TABLE II
Suitable calibration sets for identifying the MT-parameters

Calibration sets	Calibration motions						CPU time (mean)
	Gait	Squat	Stair descent	Stair ascent	Sit-to-stand-to-sit	Squat jump	
A	x				x	x	17min
B	x	x			x	x	26min
C	x			x	x	x	22min
D	x	x	x	x	x		34min
E	x	x	x		x	x	41min
F	x	x		x	x	x	37min
G	x		x	x	x	x	31min
Reference	x	x	x	x	x	x	53min

Calibration sets A-G satisfied both criteria to identify the MT-parameters of the knee actuators for all 11 datasets. The CPU time, averaged over all 11 datasets, required to solve the optimal estimation problem from both initial guesses of static parameters is given for the different suitable calibration sets.

IV. Discussion

First, we presented an optimal control problem formulation to estimate subject-specific MT-parameters of the knee actuators based on an EMG-driven model (EDM). Second, we identified several datasets containing the necessary information to estimate MT-parameters of the knee actuators.

The use of subject-specific MT-parameters rather than anthropometry-based scaled MT-parameters improved the fit between ID- and EDM-moments for all motions (see Table 3 and example Fig. 3). This suggests that the experimental approach developed in this study results in more accurate MT-parameter estimates than its anthropometric counterparts, underlining its importance for human motion simulation studies where subject-specificity is required.

The optimal estimation problem was solved via direct collocation in about 30 CPU minutes (Table 2). Direct comparison with the literature is difficult, since the CPU time largely depends on the number of optimization parameters and is often not reported. Using direct collocation methods nevertheless typically results in shorter CPU times than other approaches such as direct shooting or genetic algorithms. Sartori *et al.* [18], for example, needed more than 20 CPU hours to estimate parameters of 34 muscles using a shooting approach with a simulated annealing algorithm.

To test the robustness of our results against the initial guess, we performed all computations using two different sets of initial static parameters: a pre-computed hot start and an arbitrary guess. The most optimal solution was then selected. The two initial guesses were very different (see Table S1 supplementary materials for details). Nevertheless, optimal cost function values were very similar (average ratio hot start to arbitrary guess 101.12 ± 5.45 %), indicating that the hot start did not outperform the arbitrary guess. The influence of the initial guess on the MT-parameter estimates was also, on average, limited although larger variabilities were observed for the tendon slack length of the BFLH and the optimal muscle fiber lengths (see Table S3 supplementary materials for details). These differences underline the need for multiple initial guesses. Future work may consider the use of a second arbitrary

TABLE III
SUMMARY OF R^2 AND RMSE BETWEEN ID- AND EDM-MOMENTS

MT-parameters		Metric	**Gait** Mean ± std	**Squat** Mean ± std	**Stair descent** Mean ± std	**Stair ascent** Mean ± std	**Sit-to-stand-to-sit** Mean ± std	**Squat jump** Mean ± std
Subject-specific	Calibration set A	R^2	0.66 ± 0.10	**0.80 ± 0.13**	**0.71 ± 0.17**	**0.79 ± 0.08**	0.79 ± 0.08	0.65 ± 0.13
		RMSE (Nm)	11.64 ± 2.64	**11.12 ± 4.17**	**12.38 ± 3.96**	**11.17 ± 2.42**	9.03 ± 1.89	16.70 ± 4.62
	Calibration set B	R^2	0.66 ± 0.11	0.83 ± 0.12	**0.73 ± 0.18**	**0.76 ± 0.10**	0.77 ± 0.09	0.66 ± 0.12
		RMSE (Nm)	11.60 ± 2.72	10.33 ± 4.23	**11.84 ± 3.89**	**11.78 ± 2.72**	9.53 ± 2.21	16.55 ± 4.82
	Calibration set C	R^2	0.66 ± 0.12	**0.80 ± 0.13**	**0.73 ± 0.17**	0.81 ± 0.08	0.80 ± 0.08	0.65 ± 0.13
		RMSE (Nm)	11.64 ± 2.85	**11.15 ± 4.29**	**12.00 ± 3.92**	10.69 ± 2.48	8.97 ± 1.86	16.70 ± 4.60
	Calibration set D	R^2	0.67 ± 0.11	0.82 ± 0.10	0.73 ± 0.20	0.83 ± 0.07	0.80 ± 0.08	**0.59 ± 0.16**
		RMSE (Nm)	11.57 ± 2.64	10.52 ± 3.52	11.71 ± 3.92	10.12 ± 2.35	8.82 ± 2.07	**18.09 ± 5.55**
	Calibration set E	R^2	0.66 ± 0.11	0.82 ± 0.13	0.75 ± 0.18	**0.78 ± 0.09**	0.78 ± 0.08	0.66 ± 0.12
		RMSE (Nm)	11.67 ± 2.82	10.49 ± 4.38	11.29 ± 3.58	**11.46 ± 2.83**	9.34 ± 2.09	16.49 ± 4.73
	Calibration set F	R^2	0.67 ± 0.11	0.82 ± 0.11	**0.70 ± 0.21**	0.81 ± 0.08	0.79 ± 0.08	0.65 ± 0.14
		RMSE (Nm)	11.47 ± 2.77	10.50 ± 3.76	**12.38 ± 4.19**	10.75 ± 2.50	9.22 ± 2.13	16.85 ± 4.81
	Calibration set G	R^2	0.66 ± 0.12	**0.80 ± 0.13**	0.77 ± 0.14	0.81 ± 0.08	0.80 ± 0.09	0.65 ± 0.13
		RMSE (Nm)	11.70 ± 2.82	**11.30 ± 4.10**	11.14 ± 3.26	10.52 ± 2.25	8.90 ± 1.76	16.72 ± 4.70
Reference		R^2	0.66 ± 0.12	0.82 ± 0.13	0.74 ± 0.20	0.81 ± 0.08	0.79 ± 0.08	0.65 ± 0.13
		RMSE (Nm)	11.65 ± 2.78	10.63 ± 4.26	11.59 ± 3.91	10.76 ± 2.44	9.08 ± 1.86	16.76 ± 4.79
Linearly scaled		R^2	**0.54 ± 0.11**	**0.47 ± 0.28**	**0.71 ± 0.12**	**0.68 ± 0.12**	**0.60 ± 0.16**	**0.40 ± 0.22**
		RMSE (Nm)	**13.72 ± 3.11**	**19.96 ± 9.70**	**12.86 ± 3.31**	**14.02 ± 3.83**	**12.92 ± 4.61**	**22.41 ± 7.77**
Nonlinearly scaled		R^2	**0.54 ± 0.11**	**0.46 ± 0.28**	**0.71 ± 0.12**	**0.68 ± 0.12**	**0.60 ± 0.16**	**0.41 ± 0.22**
		RMSE (Nm)	**13.66 ± 3.10**	**20.12 ± 9.86**	**12.82 ± 3.31**	**13.98 ± 3.84**	**12.98 ± 4.65**	**22.41 ± 7.97**

A larger R^2/smaller RMSE value represents a better fit. EDM-moments are simulated based on subject-specific MT-parameters estimated from the suitable calibration sets A-G (Table 2), reference MT-parameters, linearly scaled MT-parameters, and nonlinearly scaled MT-parameters. Distinction is made between calibration motions and validation motions (in bold). Results are averaged over all 11 datasets (mean and standard deviation).

guess instead of the hot start to avoid the associated computational costs.

The variability of subject-specific tendon slack length estimates of the biceps femoris long head and subject-specific optimal muscle fiber length estimates of the rectus femoris among the seven suitable calibration sets was rather high. Further analysis nonetheless showed that these parameters had a relatively low effect on the knee moments. Therefore, we consider to keep those parameters constant in future work. Overall, subject-specific MT-parameters were comparable to anthropometry-based scaled MT-parameters for the extensors, in particular the vasti, but not for the flexors (see example Fig. 4). Further analysis showed that anthropometry-based scaled MT-parameters of the flexors, in particular the gastrocnemii and the semimembranosus, were often outside the range of physiologically feasible combinations of MT-parameters, which might provide insight in why anthropometry-based scaled MT-parameters resulted in worse moment simulations. Two explanations may explain why these MT-parameters are outside this range. First, the physiologically feasible combinations may be inappropriately defined. Their definition relied on the assumption that muscles can actively generate force at maximal and minimal MT-lengths encountered across the functional motions. These MT-lengths may however correspond to positions where the muscle cannot actively produce force, invalidating the approach. Second, an anthropometry-based scaling of the MT-parameters may not be suitable for some muscles. Delp and Zajac [37] reported that muscle forces developed by ankle plantarflexors, such as the gastrocnemii, are extremely sensitive to changes in tendon

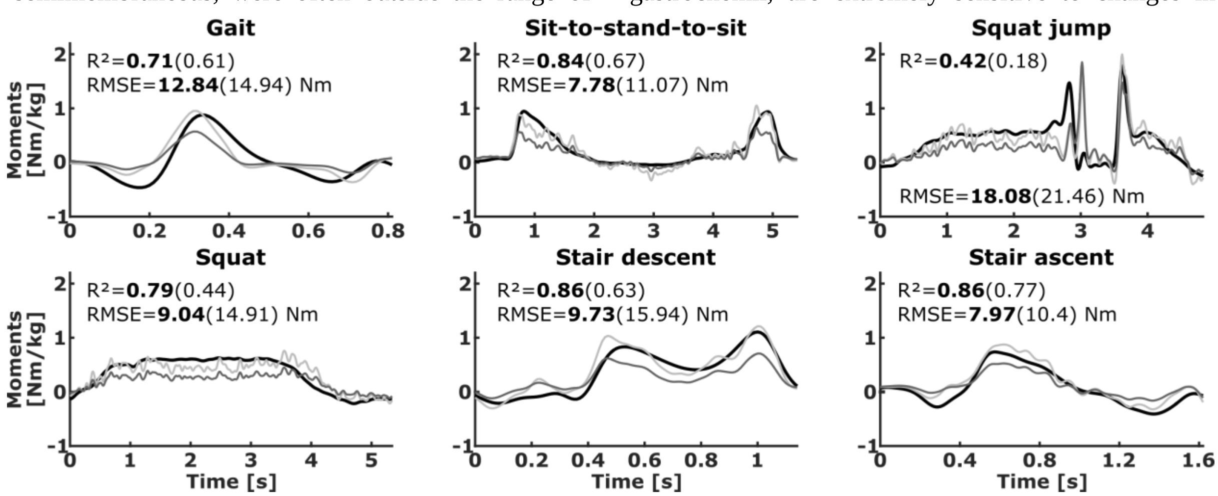

Fig. 3. Comparison between ID- (thick black) and EDM-moments simulated based on subject-specific MT-parameters (light grey) and linearly scaled MT-parameters (dark grey). This representative example from one dataset shows how the use of subject-specific MT-parameters, estimated from a suitable calibration set (top, calibration motions: gait, sit-to-stand-to-sit, squat jump), improves moment predictions for validation motions: squat, stair descent, stair ascent (bottom). Using subject-specific MT-parameters (**in bold**) instead of linearly scaled MT-parameters (between brackets) results in larger R^2 and smaller RMSE for all motions.

This article has been accepted for publication in a future issue of this journal, but has not been fully edited. Content may change prior to final publication. Citation information: DOI 10.1109/TBME.2016.2630009, IEEE Transactions on Biomedical Engineering

length. Scaling the MT-parameters of the gastrocnemii based on the subject's anthropometry might therefore have a large effect on muscle forces and corresponding muscle fiber lengths, which would exclude them from the physiologically feasible combinations. The second explanation is more likely than the first one based on the increased accuracy of moment simulations obtained with subject-specific versus anthropometry-based scaled MT-parameters. Future work will further investigate both explanations.

Studying the identifiability of the MT-parameters based on different sets of motions allowed us to determine which sets of motions contain the necessary information to identify the MT-parameters. This identifiability study was essential to ensure the estimation of parameters that describe the subject's MT-properties and could therefore be used in "what if" studies where novel motions are predicted or to calculate MT-force distributions. The subject-specific MT-parameters were estimated and validated using a rich dataset, including a wide variety of functional motions. In particular, a validation was performed by extrapolating to novel motions (i.e. motions not used in the estimation). The estimated subject-specific MT-parameters are thus expected to be valid for a wide variety of motions, including motions that were not included in this study. Without such a validation, the use of MT-parameters estimated based on functional motions should not be extrapolated to other motions and the computed MT-force distributions should be interpreted with care. We identified seven sets of motions that were suitable to identify the MT-parameters over all datasets (Table 2). Information from gait and sit-to-stand-to-sit was essential as those motions were part of all suitable calibration sets. Their sole combination was however not sufficient for four out of eleven datasets. Combining as few as three motions (calibration set A: gait, sit-to-stand-to-sit, squat jump) was sufficient for all datasets. Performing a squat jump may however be difficult in a clinical context (e.g. patients with cerebral palsy). In that case, calibration set D, containing all motions but squat jump, is a good alternative. All other suitable sets of motions were extensions of calibration set A. Although adding additional motions to calibration set A resulted in a slight increase in accuracy (∼1 %) based on R^2 and RMSE, their use required on average three times higher CPU times and additional time-consuming measurements. These findings provide guidelines about which measurements to perform and combine to estimate the MT-parameters of the knee actuators. A choice can be made based on the subject's functional abilities and the available equipment. Future research should extend this study to other motions that are more easily achievable in a clinical context and that require no or little equipment.

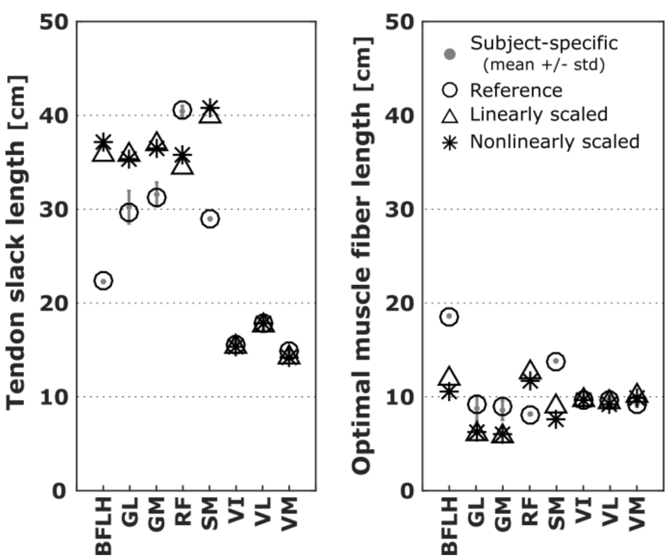

Fig. 4. Comparison between subject-specific MT-parameters averaged over the seven suitable calibration sets (grey), reference MT-parameters (circles), linearly scaled MT-parameters (triangles) and nonlinearly scaled MT-parameters (stars). This example is given for one representative dataset (subject's height, 175 cm) (see supplementary materials Fig. S3. for other datasets).

The selection of optimization parameters was driven by the need to balance accuracy of the model and available experimental information. Based on existing sensitivity studies [11], [16], [17], only a limited number of MT-parameters was optimized. These studies, however, only considered a range of parameter values from control subjects. Deviations from this range in the presence of musculoskeletal disorders may require the inclusion of additional parameters. In patients with muscle weakness it may, for example, be necessary to adjust $F_m^{\max}$ whereas this is not the case for healthy controls. Estimating a different set of parameters necessitates an analysis similar to the one presented in this study to determine whether the available experimental data contain enough information. A single optimization parameter for all muscles was used in the EMG-to-activation relationship. It is expected that including muscle-specific shape factors may result in better moment simulations [17] as it may better reflect the muscle physiology [38]. This would, however, considerably increase the number of optimization parameters and thus the risk of overfitting. Similarly, a fixed electromechanical delay (40 ms) was introduced whereas muscle- and motion-specific electromechanical delays are anticipated to result in better moment simulations.

The use of more physiologically correct models is expected to result in better moment simulations [17] and may therefore increase the MT-parameter estimation accuracy. Future research may therefore consider the inclusion of additional muscle features such as multiple muscle fiber types to better represent the motor unit recruitment strategies [39]. Muscle fatigue [40] and history-dependence [41] may also be considered. A balance between model complexity and numerical aspects is, however, needed to maintain a high computational efficiency. The model outcomes also depend on the quality of the EMG signals and the number of muscle groups from which EMG signals are extracted. On the one hand, the quality of the EMG signals is deteriorated by noise from cross-talk or movement artifacts and is affected by the envelope extraction procedure [42]. On the other hand, the collection of EMG signals from more muscle groups is expected to better represent the individual muscle contributions to the joint moments. In this study, the assignment of EMG envelopes to the model's knee actuators mainly followed common practice from the literature [17], [18]. The gastrocnemius lateralis EMG was further assumed to drive the

This article has been accepted for publication in a future issue of this journal, but has not been fully edited. Content may change prior to final publication. Citation information: DOI 10.1109/TBME.2016.2630009, IEEE Transactions on Biomedical Engineering

gastrocnemius medialis whereas the hamstring medialis EMG was assumed to drive the sartorius and gracilis. The first assumption was supported by the fact that the gastrocnemii share the same tendon and have a common knee flexion function. Experimental data are thus expected to contain information about their common function and not about their individual muscle contributions to the knee moments. The MT-parameters of those muscles will thus be estimated to provide the expected knee flexion moments. Inaccuracies in the EMG envelopes are therefore anticipated to have a small influence on this estimation. Regarding the second assumption, the sartorius and gracilis have the smallest cross sectional areas among the hip and knee muscles [18] and inaccuracies in their EMG envelopes are hence expected to have a very limited impact on the knee moment predictions. Furthermore, the MT-parameters of the sartorius and gracilis were not estimated due to their low sensitivity [11]. For those different reasons, we did not consider the use of other approaches, such as hybrid EMG-informed models [18], [42], to estimate the EMG of those three muscles. Overall, we were able to estimate subject-specific MT-parameters based on surface EMG signals from six muscle groups that improved the accuracy of knee moment predictions for novel motions. Therefore, EMG-driven models are useful even in the absence of EMG data from presumably agonistic and smaller muscles.

Sartori *et al.* [18] investigated the limitations associated with the use of EDMs that constrain MT-actuators to satisfy joint moments with respect to a single DOF. They reported discrepancies in the MT-force distribution of several bi-articular muscles (gracilis, semitendinosus, sartorius, rectus femoris and both gastrocnemii) when simulated from different single-DOF EDMs. Their findings, however, do not affect the validity of our results. First, in this study, the gracilis, semitendinosus, and sartorius were not included in the calibration process because of the low sensitivity of knee moments to MT-parameters of those muscles [16]. Second, the variations in the MT-force distribution of the rectus femoris when estimated from knee- versus hip-based EDMs in the study of Sartori *et al.* [18] might be caused by omitting active contributions of psoas and illiacus whose electrical activity could not be measured via surface EMG. This omission impacts the MT-force distribution of other hip actuators, such as the rectus femoris, when simulated using hip-based EDMs and may explain the differences with the MT-force distribution obtained using knee- based EDMs. Third, as stated above, the gastrocnemii have a common knee flexion function and experimental data are thus expected to contain information about their common function, preventing independent estimation of their MT-parameters. Note that, for this reason, an additional constraint was imposed in the optimal estimation problem (14). Discrepancies in MT-force distribution are therefore expected for these two muscles when simulated from ankle- versus knee-based EDMs while the combined MT-force distribution is anticipated to be similar. Overall, using a model that considers a sole DOF is suitable if the MT-parameters are selected so that the information needed for their estimation is available in the experimental dataset.

This study has several limitations. First, a sole DOF was considered, limiting the number of muscles included in the analysis. Extending this research to other DOFs is necessary to consider muscles spanning other joints. This nevertheless would require an identifiability study to assess whether the available experimental data contain enough information to estimate the additional parameters. Second, a limited number of functional motions was used to estimate and validate the MT-parameters. Motions not considered in the current study might provide more information. In particular, the inclusion of maximal isometric contraction trials may be beneficial although, as mentioned in the introduction, several limitations arise when using isometric dynamometry. Overall, combinations of the considered motions were suitable to obtain valid estimates of MT-parameters. Third, only sagittal plane motions were included in this study. While we could provide valid MT-parameters for these motions, extrapolation to motions in the other planes should be performed with care. Fourth, the approach for computing the moment arms is an approximation for bi-articular muscles as contact forces between joint and muscles are ignored [43]. This may therefore affect the results. In the future, the use of via-point wrapping and wrapping system [44] will be considered. Finally, no passive motions were included in the experimental datasets. Therefore, passive MT-properties cannot be estimated based on the proposed dataset.

V. Conclusion

This study proposed a new and computationally efficient optimal control problem formulation to estimate subject-specific Hill model MT-parameters of the knee actuators based on an EMG-driven model. In addition, an identifiability study was performed and underlined the importance of the selection of experimental data to provide valid estimates of MT-parameters and to prevent overfitting. Our results demonstrated the need to use subject-specific MT-parameters to obtain accurate knee moment simulations and highlighted the limitations associated with the use of anthropometric approaches to scale the MT-parameters of the knee flexors. In the future, we will extend this research to patients (e.g. children with cerebral palsy), considering their various neuromuscular impairments and their diminished abilities to perform certain motions.

References

[1] F. E. Zajac, "Muscle and tendon: properties, models, scaling, and application to biomechanics and motor control," *Crit. Rev. Biomed. Eng.*, vol. 17, no. 4, pp. 359–411, 1989.

[2] S. L. Delp et al., "An interactive gaphics-based model of the lower extremity to study orthopaedic surgical procedures," *IEEE T. Biomed. Eng.*, vol. 37, no. 8, pp. 757 – 67, 1990.

[3] M. D. Klein Horsman et al., "Morphological muscle and joint parameters for musculoskeletal modelling of the lower extremity," *Clin. Biomech.*, vol. 22, no. 2, pp. 239–247, 2007.

[4] E. M. Arnold et al., "A model of the lower limb for analysis of human movement," *Ann. Biomed. Eng.*, vol. 38, no. 2, pp. 269–279, 2010.

[5] C. R. Winby et al., "Evaluation of different analytical methods for subject-specific scaling of musculotendon parameters," *J. Appl. Biomech.*, vol. 41, no. 8, pp. 1682–1688, 2008.

[6] L. Modenese et al., "Estimation of musculotendon parameters for scaled and subject specific musculoskeletal models using an optimization technique," *J. Biomech.*, vol. 49, no. 2, pp. 141–148, 2016.

[7] R. A. Brand et al., "The sensitivity of muscle force predictions to changes in physiologic cross-sectional area," *J. Biomech.*, vol. 19, no. 8, pp. 589–596, Dec. 1986.

[8] J. A. Friederich and R. A. Brand, "Muscle fiber architecture in the human lower limb," *J. Biomech.*, vol. 23, no. 1, pp. 91–95, Jan. 1990.

[9] C. Y. Scovil and J. L. Ronsky, "Sensitivity of a Hill-based muscle model to perturbations in model parameters," *J. Biomech.*, vol. 39, no. 11, pp. 2055–2063, 2006.

[10] C. Redl et al., "Sensitivity of muscle force estimates to variations in muscle–tendon properties," *Hum. Movement Sci.*, vol. 26, no. 2, pp. 306–319, 2007.

[11] F. De Groote et al., "Sensitivity of dynamic simulations of gait and dynamometer experiments to hill muscle model parameters of knee flexors and extensors," *J. Biomech.*, vol. 43, no. 10, pp. 1876–1883, 2010.

[12] D. C. Ackland et al., "Sensitivity of model predictions of muscle function to changes in moment arms and muscle-tendon properties: A Monte-Carlo analysis," *J. Biomech.*, vol. 45, no. 8, pp. 1463–1471, Dec. 2012.

[13] M. A. King and M. R. Yeadon, "Determining subject-specific torque parameters for use in a torque-driven simulation model of dynamic jumping," *J. Appl. Biomech.*, vol. 18, no. 3, pp. 207–217, 2002.

[14] H. Hatze, "Estimation of myodynamic parameter values from observations on isometrically contracting muscle groups," *Eur. J. Appl. Physiol. O.*, vol. 46, no. 4, pp. 325–338, 1981.

[15] B. A. Garner and M. G. Pandy, "Estimation of musculotendon properties in the human upper limb," *Ann. Biomed. Eng.*, vol. 31, pp. 207–220, 2003.

[16] A. Van Campen et al., "A new method for estimating subject-specific muscle-tendon parameters of the knee joint actuators: a simulation study," *Int. J. Numer. Meth. Biomed. Engng.*, vol. 30, no. 10, pp. 969–987, 2014.

[17] D. G. Lloyd and T. F. Besier, "An EMG-driven musculoskeletal model to estimate muscle forces and knee joint moments in vivo," *J. Biomech.*, vol. 36, no. 6, pp. 765–776, Jun. 2003.

[18] M. Sartori et al., "EMG-driven forward-dynamic estimation of muscle force and joint moment about multiple degrees of freedom in the human lower extremity," *PLoS One*, vol. 7, no. 12, pp. 1–11, 2012.

[19] N. Babault et al., "EMG activity and voluntary activation during knee-extensor concentric torque generation," *Eur. J. Appl. Physiol.*, vol. 86, no. 6, pp. 541–547, 2002.

[20] M. Wesseling et al., "Subject-specific musculoskeletal modelling in patients before and after total hip arthroplasty," *Comput. Methods Biomech. Biomed. Engin.*, vol. 19, no. 15, pp. 1683–1691, 2016.

[21] S. C. White and D. A. Winter, "Predicting muscle forces in gait from EMG signals and musculotendon kinematics," *J. Electromyogr. Kines.*, vol. 2, no. 4, pp. 217–231, 1992.

[22] J. T. Betts, "Parameter estimation," in *Practical Methods for Optimal Control and Estimation Using Nonlinear Programming*, 2nd ed., Philadelphia: SIAM, 2010, ch 5, pp. 219–245.

[23] M. Ackermann and A. J. van den Bogert, "Optimality principles for model-based prediction of human gait," *J. Biomech.*, vol. 43, no. 6, pp. 1055–1060, 2010.

[24] F. De Groote et al., "A physiology-based inverse dynamic analysis of human gait using sequential convex programming: a comparative study," *Comput. Methods Biomech. Biomed. Engin.*, vol. 15, no. 10, pp. 1093–1102, 2012.

[25] F. De Groote et al., "Evaluation of direct collocation optimal control problem formulations for solving the muscle redundancy problem," *Ann. Biomed. Eng.*, 2016.

[26] F. C. Anderson and M. G. Pandy, "Dynamic optimization of human walking.," *J. Biomech. Eng.*, vol. 123, no. 5, pp. 381–390, 2001.

[27] T. S. Buchanan et al., "Neuromusculoskeletal modeling: estimation of muscle forces and joint moments and movements from measurements of neural command," *J. Appl. Biomech.*, vol. 20, no. 4, pp. 367–395, 2004.

[28] P. Konrad, "The ABC of EMG," *A practical introduction to kinesiological electromyography*, 1st ed, 2005, pp. 1–60.

[29] S. L. Delp et al., "OpenSim: open-source software to create and analyze dynamic simulations of movement," *IEEE T. Biomed. Eng.*, vol. 54, no. 11, pp. 1940–1950, 2007.

[30] M. H. Schwartz and A. Rozumalski, "A new method for estimating joint parameters from motion data," *J. Biomech.*, vol. 38, no. 1, pp. 107–116, 2005.

[31] F. De Groote et al., "Kalman smoothing improves the estimation of joint kinematics and kinetics in marker-based human gait analysis," *J. Biomech.*, vol. 41, no. 16, pp. 3390–3398, 2008.

[32] D. G. Thelen, "Adjustment of muscle mechanics model parameters to simulate dynamic contractions in older adults," *J. Biomech. Eng.*, vol. 125, no. 1, pp. 70–77, 2003.

[33] J. M. Winters, "An improved muscle-reflex actuator for use in large-scale neuromusculoskeletal models," *Ann. Biomed. Eng.*, vol. 23, no. 4, pp. 359–374, 1995.

[34] M. A. Patterson and A. V. Rao, "GPOPS − II : a MATLAB software for solving multiple-phase optimal control problems using hp – adaptive Gaussian quadrature collocation methods and sparse nonlinear programming," *ACM T. Math. Software*, vol. 41, no. 1, pp. 1:1–1:37, 2014.

[35] A. Wächter and L. T. Biegler, "On the implementation of an interior-point filter line-search algorithm for large-scale nonlinear programming," *Math. Program.*, vol. 106, no. 1, pp. 25–57, 2006.

[36] M. J. Weinstein and A. V. Rao, "A source transformation via operator overloading method for the automatic differentiation of mathematical functions in MATLAB," *ACM T. Math. Software*, vol. 42, no. 2, p. 44, 2016.

[37] S. L. Delp and F. E. Zajac, "Force- and moment generating capacity of lower extremity muscles before and after tendon lengthening," *Clin. Orthop. Relat. Res.*, vol. 284, pp. 247–259, 1992.

[38] J. J. Woods and B. Bigland-Ritchie, "Linear and non-linear surface EMG/force relationships in human muscles. An anatomical/functional argument for the existence of both," *Am. J. Phys. Med.*, vol. 62, no. 6, pp. 287–299, Dec. 1983.

[39] J. M. Wakeling et al., "A muscle's force depends on the recruitment patterns of its fibers," *Ann. Biomed. Eng.*, vol. 40, no. 8, pp. 1708–1720, 2012.

[40] B. R. Umberger et al., "A model of human muscle energy expenditure," *Comput. Methods Biomech. Biomed. Engin.*, vol. 6, no. 2, pp. 99–111, 2003.

[41] V. M. Zatsiorsky and B. I. Prilutsky, *Biomechanics of Skeletal Muscles*. Champaign: Human Kinetics, 2012.

[42] M. Sartori et al., "Hybrid neuromusculoskeletal modeling to best track joint moments using a balance between muscle excitations derived from electromyograms and optimization," *J. Biomech.*, vol. 47, no. 15, pp. 3613–3621, 2014.

[43] M. A. Sherman et al., "What is a moment arm? Calculating muscle effectiveness in biomechanical models using generalized coordinates," in *ASME/IDETC/CIE*, Portland, OR, 2013, pp. 1–9.

[44] A. Scholz et al., "A fast multi-obstacle muscle wrapping method using natural geodesic variations," *Multibody Syst. Dyn.*, vol. 36, no. 2, pp. 195–219, 2016.